What to do when the F10.7 goes out?

Sean Elvidge[1], David R. Themens[1], Matthew K. Brown[1] & Elizabeth Donegan-Lawley[1]
[1]Space Environment Research Group (SERENE), University of Birmingham, UK

Key Points

1. The F10.7 index is a critical value used in modelling of the upper atmosphere
2. If the index is unavailable the closest way to reconstruct it is by using solar radio fluxes at other wavelengths
3. Sunspot number can also reconstruct F10.7 but rotation, 12-month running mean, nor using a fixed value do not provide good approximations

Abstract

The solar radio flux at 10.7 cm, known as F10.7, is a critical operational space weather index. However, without a clear backup, any interruption to the service can result in substantial errors in model outputs. In this paper we show the impact of one such outage in March 2022 and present a number of alternative solutions for any future outages. The approach resulting in the smallest reconstruction error of F10.7 uses the solar radio flux observations at alternative wavelengths (the best giving a percentage error of 3.1%). Alternatively, use of Sunspot Number, a regular, robust alternative observation, results in a mean percentage error of 8.2% and is also a reliable fallback solution. Additionally, analysis of the error on the use of the conversion between the 12-month rolling sunspot number (R12) and its conversion to F10.7 as used by the IRI is included.

Plain Language Summary

Models of the upper atmosphere rely on a variety of indices and drivers to run; one of the most common is a measurement of the 10.7 cm radio wavelength flux from the Sun, known as the F10.7. It has been continuously measured in Canada since 1947, and this long record makes it an excellent index for investigating upper atmosphere variations over a wide range of timescales. However, even though the index is used operationally at many space weather centres, there are currently no backup or alternative direct observations of F10.7. This paper describes a number of alternative observations which can be used to "fill in" for the F10.7 should there be a break in the observations, as there was in March 2022.

Introduction

The solar radio flux at 10.7 cm, known as F10.7, is one of the most commonly used indices of solar activity. It is used to drive both statistical and first principles models of the ionosphere and thermosphere and finds use in a wide range of applications spanning radio communications and navigation modelling (e.g. Warrington (2009), ITU-R P.2297-0 (2013), Datta-Barua (2014), Themens and Jayachandran (2016)), remote sensing (e.g. Yeo et al. (2015), Ruck and Themens (2021), Thomas and Shepherd (2022)), solar physics (Tapping and Morgan (2017), Brooks et al. (2017)), and space environment climate and modelling (Matthes et al. (2017), Chapman et al. (2018), Kodikara et al. (2018), Elvidge and Angling (2019), Nugent et al. (2020), Bilitza et al. (2022)). F10.7 is a proxy for the solar extreme ultraviolet (EUV) forcing of the upper atmosphere and has been measured since 1947 (K. F. Tapping, 2013). Each reported F10.7 value is an observation of the total radio emission in a 100 MHz-wide channel centred at 2800 MHz (wavelength of 10.7 cm) from all sources on the solar disk. Three of these flux density observations are made each day, at 1700, 2000, and 2300 UT (except during winter when the times are 1800, 2000, and 2200 UT). The observation is expressed in solar flux units (sfu), where $1\ \text{sfu} = 10^{-22}\ \text{Wm}^{-2}\text{s}$.

The use of F10.7 in such a broad range of models, from research to operations, can at least partially be ascribed to the fact that it is a stable, long-term, ground-based observation that has been used to investigate variations over a wide range of timescales (Dudok de Wit & Bruinsma, 2017). From 1947 to 1991 the F10.7 was measured in Ottawa, Canada when the site was moved to the Dominion Radio Astrophysical Observatory (DRAO) in Penticton, Canada. The DRAO, which provides the F10.7 data freely to the community, is supported by National Research Council (NRC) of Canada in partnership with Natural Resources Canada (NRCan). This data stream is used globally for operational space weather products including those from the US Space Weather Prediction Center and the UK Met Office Space Weather Operations Centre. Thus, it is critical for operational space environment monitoring, forecasting, and mitigation services. However, this critical reliance of a wide variety of operational systems on a steady stream of F10.7 measurements poses a risk to the performance of these systems, should the F10.7 data stream be interrupted, particularly if such an interruption lasts more than a few days.

Such an interruption occurred on March 18th, 2022, when a cyberattack caused a network interruption at the NRC, which resulted in an F10.7 outage that lasted over a month. Without redundant systems, many critical space weather architectures suddenly become unavailable, or, perhaps worse, generate output using "default values" of F10.7 (for example an F10.7 of 100) which can also be used for forcings in forecasts, potentially producing substantial errors without suitable warnings. For example, both the International Reference Ionosphere (Bilitza et al., 2022) and the Empirical Canadian High Arctic Ionospheric Model (Themens et al., 2017) immediately revert to the use of NOAA long-term F10.7 forecasts if measured values are not available. On March 18th, 2022, resorting to these forecasts constituted an immediate error of ~14 sfu, increasing to an error of ~70 sfu just ten days later as an active region rotated onto the disk.

In this study we explore the impacts of having to mitigate the F10.7 interruption experienced in March 2022 using a number of methods and investigate their suitability as an F10.7 redundancy.

Models

In addition to DRAO in Canada, the other notable observatory which records solar radio flux is the Nobeyama Radio Observatory in Japan (previously recorded in Toyokawa from 1951 to 1994), operated by the National Astronomical Observatory of Japan (https://solar.nro.nao.ac.jp/norp/), which makes continuous observations of flux densities at wavelengths of 30 cm, 15 cm, 8 cm and 3.2 cm (Tanaka et al., 1973). The 30 cm flux (from herein called F30) can be used by the Drag Temperature Model (DTM) and Dudok de Wit and Bruinsma (2017) argue that it is more sensitive than the 10.7 cm flux to longer wavelengths in the UV. Whilst the Nobeyama observatory does not observe the F10.7 flux density, which many space weather models require, the wavelengths measured can be used to generate a proxy for F10.7. A simple expression using just the observation at 15 cm (from herein called F15), which is the observation best correlated with the F10.7, can be found using non-linear least squares to low-order polynomials. For example, by fitting all available data, spanning November 1951 to November 2022, to a second-order polynomial, we find the following expression for adjusted F10.7 using F15:

$$F10.7_{F15} = 0.00093 \cdot F15^2 + 0.97 \cdot F15 + 15.43. \quad (1)$$

This results in an average root mean square error, compared to the measured F10.7, of ~7 sfu. This can be further reduced to ~6 sfu using a more complicated expression that also incorporates F8 (solar flux at 8 cm wavelength):

$$F10.7_{F15F8} = 0.00054 \cdot F15^2 + 0.25 \cdot F15 - 0.0012 \cdot F8^2 + 0.85 \cdot F8 + 0.0012 \cdot F15 \cdot F8 - 8.67. \quad (2)$$

Both expressions enable a value of F10.7 to be used in case of an outage at the Penticton observatory, using observations from Nobeyama.

Additionally, the Collecte Localisation Satellites (CLS) group in France provide a routinely updated file (https://spaceweather.cls.fr/services/radioflux/) of both the absolute observations and 1 AU corrected observations of F3.2, F8, F15, and F30. This file also contains the observed and interpolated values of F10.7, where an (undescribed) method is used to fill in missing or poor quality F10.7 flux data using measurements at the other solar flux wavelengths. It should be noted that since 1 May 2018, the F10.7 in the CLS database is entirely composed of interpolated values rather than measurements since they gather their F10.7 from the no longer supported NOAA repository which was last updated in May 2018.

More commonly used approaches to estimate F10.7, rather than using additional solar radio flux wavelengths, concern the sunspot number (SN) (Clette, 2021). Historically, a wide range of formulae have been used to describe the relationship between F10.7 and SN. Tables 1 and 2 in Clette (2021) describe 18 such formulae, based on either version 1 (SN_{v1}) or version 2 (SN_{v2}) of the Sunspot Number (Clette et al., 2014; Clette & Lefèvre, 2016). Clette (2021) also describes a new high-degree polynomial fit using SN_{v2} given by:

$$F10.7_{Clette} = 1.225 \times 10^{-8} SN_{v2}^4 - 1.033 \times 10^{-5} SN_{v2}^3 + 2.613 \times 10^{-3} SN_{v2}^2 + 0.3938 SN_{v2} + 69.41. \quad (3)$$

One equation that was not presented in Clette (2021), which uses the 12-month running SN_{v1} ($R12_{v1}$), is perhaps the most commonly used equation amongst all of them and is the ITU-R Recommendation (ITU-R P.371-8, 1999):

$$F10.7_{ITU} = 0.00089 \cdot R12_{v1}^2 + 0.728 \cdot R12_{v1} + 63.7. \quad (4)$$

This equation is used in both the International Reference Ionosphere (IRI) model (Bilitza et al., 2017) and NeQuick (Nava et al., 2008), as well as in a variety of other places. However, seemingly like the child's game 'Telephone' a key term has been lost from Equation 4, $F10.7_{12}$. The equation was originally designed as a relationship between R12 and the 12-month running mean of F10.7, $F10.7_{12}$, not as a relationship to F10.7 directly (Bilitza, 1990). This misuse may be in part explained by the fact that the relationship in Equation 4 provides a slightly better fit (smaller standard deviation of errors) to the daily F10.7 than the equation specifically designed for that purpose ($F10.7_{CCIR} = 23e^{-0.05R12_{v1}} + R12_{v1} + 46$) also given in Bilitza (1990).

It is important to note that Equation 4, is still used by the IRI and NeQuick, but must use SN_{v1} since the internal empirical relationships were developed with that version of the SN. However, SN_{v1} is no longer produced and the recorded values must be 'converted' back to version 1. Currently this is done using the ratio

$$SN_{v2} = \frac{SN_{v1}}{0.6 \times 1.177} = \frac{SN_{v1}}{0.7062}, \quad (5)$$

where the 0.6 is due to the change of reference observer and the 1.177 is to offset an inflation factor in the original SN values since 1946 (Clette, 2021). The relationship between SN_{v2} and SN_{v1} is roughly linear, and more complex expressions do not significantly reduce the root mean square error (RMSE) between the version 2 and version 1 conversion of approximately 6.2 sunspots.

The use of Equation 4 is not a problem in NeQuick as users input an F10.7 value that is then converted to $R12_{v1}$; however in the IRI, both F10.7 and $R12_{v1}$ are required by various submodules

(e.g. F10.7 used by Danilov et al. (1995), Shubin (2015), Fejer et al. (2008) and $R12_{v2}$ by Altadill et al. (2013) and Scotto et al. (1997) [for a complete list see Table 8 of Bilitza et al. (2022)]). Returning to our previous example of the behaviour of the IRI during the March 2022 F10.7 interruption, one could attempt to mitigate the errors caused by the reversion to the NOAA F10.7 forecast by applying one of the many relationships above to determine a synthetic F10.7 that could be manually inputted with the model call. If the IRI is run with no specified options it will use $R12_{v2}$ and F10.7 from its internal databases, convert $R12_{v2}$ to $R12_{v1}$ using Equation 5, and run the model. However users can directly specify F10.7 and/or $R12_{v2}$. If only one is provided then the other is calculated using Equations 4 and 5. This enables the IRI to mitigate against an F10.7 interruption through the use of R12; however, this behaviour results in a mean absolute percentage error of 14.3% in the F10.7 that will be used in the model; as such, users should eliminate this error when driving the IRI with user inputs by passing both the $R12_{v2}$ and F10.7. During an F10.7 outage, other methods, as we will show in the following section, can provide much greater performance than relying on the simple internal relationship to R12.

Results

During the outage, the observed F10.7 changed by over 50 flux units, an increase of more than 60%. To put this in context, the mean percentage change over a 30-day period is 31% (albeit with a standard deviation of 19%), meaning that the outage period in question is ~1.5 standard deviations above the average variation that we would expect over such a period. To investigate the impact the replacements for F10.7 in upper atmosphere models, the Thermosphere Ionosphere Electrodynamics General Circulation Model (TIE-GCM; (Qian et al., 2014)) has been driven with the observed F10.7 (adjusted to correct for the changing distance between the Earth and the Sun) until the outage on March 18th 2022, at which point each of the above models have been used as the F10.7 for the remaining run of TIE-GCM. All other parameters are kept the same. These have then been compared to a 'true' run using the observed F10.7 values after the outage was fixed. The F10.7 replacement models are:

1. F15 – the F10.7 derived from the 15 cm flux, Equation 1
2. F15 & F8 – the F10.7 derived from the 15 cm and 8 cm flux, Equation 2
3. Clette – the updated fourth-order polynomial estimating F10.7 from the daily SN_{v2}, Equation 3
4. $R12_{v1}$ – the ITU-R recommendation for estimating F10.7 from $R12_{v1}$ as used by, amongst others, the IRI, Equation 4
5. Constant – the F10.7 is held at a constant value of 97.8 throughout the model run, the last observation before the outage started
6. 27-Day Rotation – the value from 27 days ago is assumed as the current value

Figure 1 shows the global mean absolute percentage error of the total electron content (TEC) in the ionosphere for the six different F10.7 replacement models, as previously described. Mean absolute percentage error (MAPE) is defined as:

$$MAPE = \frac{1}{N}\sum_{i=1}^{N}\left|\frac{observation_i - truth_i}{truth_i}\right|, \quad (6)$$

for an $observation$ and $truth$ time series of length N. It is clear, and unsurprising, that the models based on closely-related other observation data, F15, F15 & F8 and Clette, do significantly better than the model based on $R12_{v1}$, a constant value and the rotation model. The largest error, of approximately 140% for the $R12_{v1}$ method, coincides with the peak of the increasing observed F10.7 on 31 March. Across the whole time period the model that uses either F15 alone (Equation 1) or both F15 and F8 (Equation 2) performs the best, slightly outperforming the Clette model at the beginning and end of the time period (with a similar performance between all three in the middle of the test period).

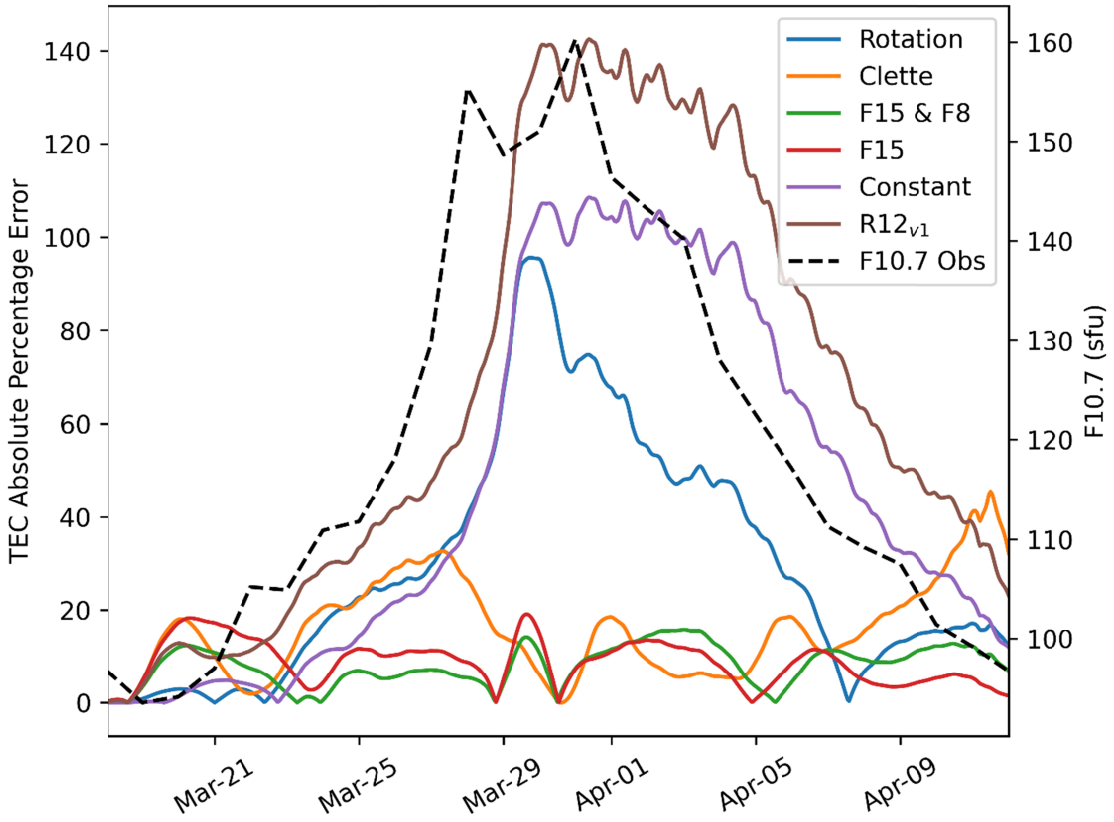

Figure 1. Absolute percentage error of total electron content (TEC) across the F10.7 outage time period in March and April 2022.

In contrast to Figure 1, which shows the overall global absolute percentage error in TEC, Figure 2 gives an example of the global TEC differences in TIE-GCM on March 27 at 1000, nine days after the outage began. It is still clear that the $R12_{v1}$, Constant, and Rotation models give the largest errors, and all of the models perform worse at the daytime equatorial anomaly.

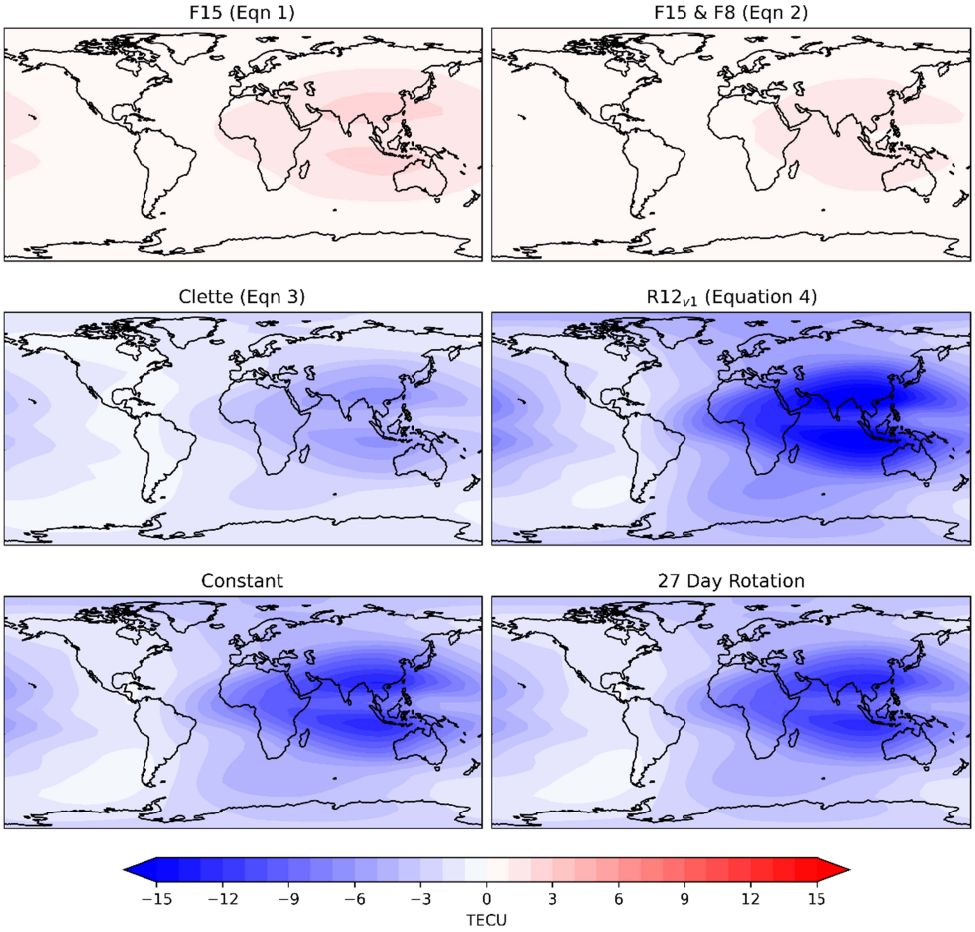

Figure 2. Error in total electron content (TEC) in TIE-GCM between using the observed F10.7 and the different F10.7 models at 1000 on March 27th.

The results presented thus far only cover the specific outage period from March and April 2022. To perform a more rigorous study of the different approaches, the error statistics of these approaches have been compared to the observed F10.7 over a 71-year period (from November 1951 to November 2022). In replacement of the 'Constant' model used previously an additional model, the average F10.7 across the 71-year time interval (120 sfu) has been used.

Table 1. Error statistics for different models for estimating F10.7

Model	**Mean Absolute Percentage Error (%)**	**Bias (sfu)**	**RMSE (sfu)**
F15 (Equation 1)	3.73	0.25	7.12
F15 & F8 (Equation 2)	3.13	0.73	6.00
Clette (Equation 3)	8.18	-0.13	15.3
R12$_{v1}$ (Equation 4)	13.9	-1.46	26.7
Average F10.7 (120 sfu)	38.5	-0.02	52.1
27-Day Rotation	11.6	-0.03	24.9

The overall error statistics shown in Table 1 are in line with the previous example, the models using additional solar flux observations at 15 cm (F15) and 8 cm (F8) wavelengths, and F15 alone,

perform best, with a mean absolute percentage error of 3.13% and 3.73% respectively. The Clette model also performs very well with ~8% error, followed by the Rotation, $R12_{v1}$ and the worse performing model (unsurprisingly) is the Average F10.7 model with a 38.5% error.

Conclusions & Discussion

The solar radio flux at 10.7 cm, F10.7, is a critical index for space weather modelling and is one of the most commonly applied indices of solar activity used to drive both statistical and first principles models of the ionosphere and thermosphere. A number of operational systems rely on the F10.7; as such, a serious risk is posed by an interruption to the F10.7 data stream. Such an interruption occurred on March 18th 2022 when the F10.7 observations could not be made available due to a cyberattack. Without any clear, redundant system, models can stop working or can rely on default values (often without providing suitable warnings).

This paper has presented a number of proxy models for F10.7, based on flux densities at 15 cm and 8 cm, sunspot number, 12-month mean sunspot number, 27-day rotations and using a fixed value. It has been shown that the use of the average F10.7, 12-month mean sunspot number and the 27-day rotation would cause significant errors in estimating F10.7 (38.5%, 13.9% and 11.6% respectively, in terms of mean absolute percentage error) and should be avoided in an operational setting if there is a loss of F10.7. The best performing models rely on using additional wavelength observations at 15 cm and 8 cm, which can be used to reconstruct F10.7 with just a 3.1% error. Using the best fitting high-order polynomial fit of sunspot number (SN_{v2}) to F10.7, as described by Clette (2021), results in an 8.2% error. Whilst this approach clearly performs worse, it has the advantage of being based on a robust observation, with recorded daily observations from 1818, making it a good choice as a redundant option for operational systems or in the backwards reconstruction of F10.7 for events prior to 1947.

Open Research

The F10.7 observations are recorded at the Dominion Radio Astrophysical Observatory, and freely provided to the space weather community with support from Natural Resources Canada. We are immensely grateful to them for their continued effort in providing this critical resource. The data daily and monthly and rotational averages can be downloaded from https://spaceweather.gc.ca/forecast-prevision/solar-solaire/solarflux/sx-5-en.php. The raw Nobeyama observations of F30, F15, F8 and F3.2 are available from https://solar.nro.nao.ac.jp/norp/data/daily/. Flare corrected, and Sun-Earth distance adjusted values are provided by Collecte Localisation Satellites (CLS) available from ftp://ftpsedr.cls.fr/pub/previsol/solarflux/observation/radio_flux_adjusted_observation.txt.
Finally, the daily Sunspot Number is provided by WDC-SILSO, Royal Observatory of Belgium, Brussels, and can be downloaded from https://www.sidc.be/silso/DATA/EISN/EISN_current.csv.

References

Altadill, D., Magdaleno, S., Torta, J. M., & Blanch, E. (2013). Global empirical models of the density peak height and of the equivalent scale height for quiet conditions. *Advances in Space Research*, *52*(10), 1756–1769. https://doi.org/10.1016/j.asr.2012.11.018

Bilitza, D. (1990). *Solar-terrestrial models and application software*. Greenbelt, Maryland: National Space Sciences Data Center, World Data Center A for Rockets and Satellites, Goddard Space Flight Center.

Bilitza, D., Altadill, D., Truhlik, V., Shubin, V., Galkin, I., Reinisch, B., & Huang, X. (2017). International Reference Ionosphere 2016: From ionospheric climate to real-time weather predictions. *Space Weather*, *15*(2), 418–429. https://doi.org/10.1002/2016SW001593
Bilitza, D., Pezzopane, M., Truhlik, V., Altadill, D., Reinisch, B. W., & Pignalberi, A. (2022). The International Reference Ionosphere Model: A Review and Description of an Ionospheric Benchmark. *Reviews of Geophysics*, *60*(4), e2022RG000792. https://doi.org/10.1029/2022RG000792
Brooks, D. H., Baker, D., van Driel-Gesztelyi, L., & Warren, H. P. (2017). A Solar cycle correlation of coronal element abundances in Sun-as-a-star observations. *Nature Communications*, *8*(1), 183. https://doi.org/10.1038/s41467-017-00328-7
Chapman, S. C., Watkins, N. W., & Tindale, E. (2018). Reproducible Aspects of the Climate of Space Weather Over the Last Five Solar Cycles. *Space Weather*, *16*(8), 1128–1142. https://doi.org/10.1029/2018SW001884
Clette, F. (2021). Is the F10.7cm – Sunspot Number relation linear and stable? *Journal of Space Weather and Space Climate*, *11*, 2. https://doi.org/10.1051/swsc/2020071
Clette, F., & Lefèvre, L. (2016). The New Sunspot Number: Assembling All Corrections. *Solar Physics*, *291*(9), 2629–2651. https://doi.org/10.1007/s11207-016-1014-y
Clette, F., Svalgaard, L., Vaquero, J. M., & Cliver, E. W. (2014). Revisiting the Sunspot Number. *Space Science Reviews*, *186*(1), 35–103. https://doi.org/10.1007/s11214-014-0074-2
Danilov, A. D., Rodevich, A. Yu., & Smirnova, N. V. (1995). Problems with incorporating a new D-region model into the IRI. *Advances in Space Research*, *15*(2), 165–168. https://doi.org/10.1016/S0273-1177(99)80042-8
Datta-Barua, S., Walter, T., Bust, G. S., & Wanner, W. (2014). Effects of solar cycle 24 activity on WAAS navigation. *Space Weather*, *12*(1), 46–63. https://doi.org/10.1002/2013SW000982
Dudok de Wit, T., & Bruinsma, S. (2017). The 30 cm radio flux as a solar proxy for thermosphere density modelling. *Journal of Space Weather and Space Climate*, *7*, A9. https://doi.org/10.1051/swsc/2017008
Elvidge, S., & Angling, M. J. (2019). Using the local ensemble Transform Kalman Filter for upper atmospheric modelling. *Journal of Space Weather and Space Climate*, *9*, A30. https://doi.org/10.1051/swsc/2019018
Fejer, B. G., Jensen, J. W., & Su, S.-Y. (2008). Quiet time equatorial F region vertical plasma drift model derived from ROCSAT-1 observations. *Journal of Geophysical Research: Space Physics*, *113*(A5). https://doi.org/10.1029/2007JA012801
ITU-R P.371-8. (1999). *ITU-R Choice of Indices for Long-Term Ionospheric Predictions, Recommendation ITU-R P. 371-8*. Retrieved from https://www.itu.int/dms_pubrec/itu-r/rec/p/R-REC-P.371-8-199907-I!!PDF-E.pdf
ITU-R P.2297-0. (2013). *Electron density models and data for transionospheric radio propagation* (P Series). Retrieved from https://extranet.itu.int/brdocsearch/R-REP/R-REP-P/R-REP-P.2297/R-REP-P.2297-2013/R-REP-P.2297-2013-MSW-E.docx
Kodikara, T., Carter, B., & Zhang, K. (2018). The First Comparison Between Swarm-C Accelerometer-Derived Thermospheric Densities and Physical and Empirical Model Estimates. *Journal of Geophysical Research: Space Physics*, *123*(6), 5068–5086. https://doi.org/10.1029/2017JA025118
Matthes, K., Funke, B., Andersson, M. E., Barnard, L., Beer, J., Charbonneau, P., et al. (2017). Solar forcing for CMIP6 (v3.2). *Geoscientific Model Development*, *10*(6), 2247–2302. https://doi.org/10.5194/gmd-10-2247-2017
Nava, B., Coisson, P., & Radicella, S. (2008). A new version of the neQuick ionosphere electron density model. *Journal of Atmospheric and Solar Terrestrial Physics*, *70*(15), 1856–1862.
Nugent, L. D., Elvidge, S., & Angling, M. J. (2020). Comparison of low-latitude ionospheric scintillation forecasting techniques using a physics-based model. *Space Weather*.
Qian, L., Burns, A. G., Emery, B. A., Foster, B., Lu, G., Maute, A., et al. (2014). The NCAR TIE-GCM: A Community Model of the Coupled Thermosphere/Ionosphere System. In J. Huba, R.

Schunk, & G. Khazanov (Eds.), *Modeling the Ionosphere-Thermosphere System* (pp. 73–83). Chichester, UK: John Wiley & Sons, Ltd. https://doi.org/10.1002/9781118704417.ch7
Ruck, J. J., & Themens, D. R. (2021). Impacts of Auroral Precipitation on HF Propagation: A Hypothetical Over-the-Horizon Radar Case Study. *Space Weather*, *19*(12), e2021SW002901. https://doi.org/10.1029/2021SW002901
Scotto, C., Mosert de González, M., Radicella, S. M., & Zolesi, B. (1997). On the prediction of F1 ledge occurrence and critical frequency. *Advances in Space Research*, *20*(9), 1773–1775. https://doi.org/10.1016/S0273-1177(97)00589-9
Shubin, V. N. (2015). Global median model of the F2-layer peak height based on ionospheric radio-occultation and ground-based Digisonde observations. *Advances in Space Research*, *56*(5), 916–928. https://doi.org/10.1016/j.asr.2015.05.029
Tanaka, H., Castelli, J. P., Covington, A. E., Krüger, A., Landecker, T. L., & Tlamicha, A. (1973). Absolute calibration of solar radio flux density in the microwave region. *Solar Physics*, *29*(1), 243–262. https://doi.org/10.1007/BF00153452
Tapping, K., & Morgan, C. (2017). Changing Relationships Between Sunspot Number, Total Sunspot Area and F10.7 in Cycles 23 and 24. *Solar Physics*, *292*(6), 73. https://doi.org/10.1007/s11207-017-1111-6
Tapping, K. F. (2013). The 10.7 cm solar radio flux (F10.7). *Space Weather*, *11*(7), 394–406.
Themens, D. R., & Jayachandran, P. T. (2016). Solar activity variability in the IRI at high latitudes: Comparisons with GPS total electron content. *Journal of Geophysical Research: Space Physics*, *121*(4), 3793–3807. https://doi.org/10.1002/2016JA022664
Themens, D. R., Jayachandran, P. T., Galkin, I., & Hall, C. (2017). The Empirical Canadian High Arctic Ionospheric Model (E-CHAIM): NmF2 and hmF2. *Journal of Geophysical Research: Space Physics*, *122*(8), 9015–9031. https://doi.org/10.1002/2017JA024398
Thomas, E. G., & Shepherd, S. G. (2022). Virtual Height Characteristics of Ionospheric and Ground Scatter Observed by Mid-Latitude SuperDARN HF Radars. *Radio Science*, *57*(6), e2022RS007429. https://doi.org/10.1029/2022RS007429
Warrington, E. M., Bourdillon, A., Benito, E., Bianchi, C., Monilié, J.-P., Muriuki, M., et al. (2009). Aspects of HF radio propagation. *Annals of Geophysics*, *52*(3–4), 301–321. https://doi.org/10.4401/ag-4577
Yeo, K. L., Ball, W. T., Krivova, N. A., Solanki, S. K., Unruh, Y. C., & Morrill, J. (2015). UV solar irradiance in observations and the NRLSSI and SATIRE-S models. *Journal of Geophysical Research: Space Physics*, *120*(8), 6055–6070. https://doi.org/10.1002/2015JA021277